Applications and Applied Mathematics: An International Journal (AAM)

Volume 18 | Issue 1 Article 5

6-2023

(R1966) Semi Analytical Approach to Study Mathematical Model of Atmospheric Internal Waves Phenomenon

Patel Yogeshwari
P D Patel Institute of Applied Sciences

Jayesh M. Dhodiya
Sardar Vallabhbhai National Institute of Technology

Available at
http://pvamu.edu/aam
Appl. Appl. Math.
ISSN: 1932-9466

Applications and Applied Mathematics:
An International Journal
(AAM)

Vol. 18, Issue 1 (June 2023), Article 5, 16 pages

Semi Analytical Approach to Study Mathematical Model of Atmospheric Internal Waves Phenomenon

[1]**Patel Yogeshwari F and** [2]**Jayesh M Dhodiya**

[1]Department of Mathematical Sciences
P D Patel Institute of Applied Sciences
Anand Gujarat 388421, India
[2]Applied Mathamtics & Humanities Department
Sardar Vallabhbhai National Institute of Technology
Surat Gujarat 395007, India
[1]patel.yogeshwari7@gmail.com; [2]jdhodiya2002@yahoo.com

*Corresponding Author: Yogeshwari Patel

Abstract

This research aims to study atmospheric internal waves which occur within the fluid rather than on the surface. The mathematical model of the shallow fluid hypothesis leads to a coupled nonlinear system of partial differential equations. In the shallow flow model, the primary assumption is that vertical size is smaller than horizontal size. This model can precisely replicate atmospheric internal waves because waves are dispersed over a vast horizontal area. A semi-analytical approach, namely modified differential transform, is applied successfully in this research. The proposed method obtains an approximate analytical solution in the form of convergent series without any linearization, perturbation, or calculation of unneeded terms, which is a significant advantage over other existing methods. To test the effectiveness and accuracy of the proposed method, obtained results are compared with Elzaki Adomain Decomposition Method, Modified Differential Transform Method, and Homotopy Analysis Method.

Keywords: Climate prediction; Shallow fluid equations (SFE); Atmospheric internal waves (AIW); coupled system of a partial differential equation; Semi-analytical approach

MSC 2010 No.: 35F55, 35F50

1. Introduction

The natural phenomena of internal waves, known as internal gravity waves, occur within a geophysical fluid rather than on its surface (such as the atmosphere, oceans, or lakes). The fluid must be layered for the phenomena to occur; each layer must have the same temperature and density, which should fluctuate with height only. The waves travel horizontally like surface waves when density changes over a small vertical height (Imani et al. (2012)). Internal waves in the atmosphere arise when a homogeneous layer of air passes over a major obstacle, such as a mountain range. Horizontal patterns of homogeneous air are disturbed when the air meets the barrier, forming a wave pattern. They can cause wave clouds, generated when steady air passes over an obstacle like a mountain. Because air mass moves through the wave, it ascends and descends repeatedly. The formation of clouds occurs at the cooled peaks of these waves if the atmosphere is humid enough. Due to adiabatic heating, such clouds will vaporize in the descendant section of the wave, resulting in the clear stripes and classic clouded. This phenomenon has been observed in several places of the world. Recent research has found that these waves significantly affect the chemistry, turbulence, and atmospheric temperature and are increasingly used in atmospheric models. Prediction of climate is a type of numerical prediction of weather that tries to give a generic climate prediction over long periods, such as a few weeks to a few years, to aid in agricultural planning, cyclone, air quality forecasting, and drought mitigation (Varsoliwala and Singh (2021)). Recent climate models used for predicting have a limited ability, using only a few day's worths of data. In such models, it is difficult to adequately reflect the intricate interactions between the land surface, ocean, and atmosphere. Climate models are systems of PDEs derived from the fundamental law of sciences, a combination of thermodynamics, chemistry, and fluid motion used to describe the atmosphere and ocean. Because the atmosphere is considered fluid, it is critical to research its properties to improve climate forecasting. Understanding how these waves work would allow for more accurate weather forecasting simulations.

The standard model depicts the occurrence of AIW waves in shallow water equations or shallow fluid equations (SFEs). The SFM primary assumption is that the vertical dimension is substantially smaller than the horizontal dimension. To model the flow of fluid in atmospheres, coastal areas, and seas, SWEs are used, a general system of coupled nonlinear partial differential equations. Shallow fluid assumptions are used to study Kelvin and Rossby waves in the atmosphere, climate, and tsunami models.

Researchers have previously addressed the internal waves phenomena from various perspectives. Imani et al. (2014) apply homotopy perturbation method (HPM) and variational iteration method to study the atmospheric internal wave model. To solve coupled linear and nonlinear shallow water equations (SWE) in one dimension, Chakraverty and Karunakar (2018, 2021) use the homotopy perturbation method. They compare the solutions of linear and nonlinear SWEs graphically. RVIM was employed by Imani et al. (2012) to study the coupled Whitham Broer Kaup equation. To solve the AIW, Busrah used Homotopy and Variational Iteration Methods. The homotopy method was successfully used by Jaharuddin and Hermansyah to determine the approximate solution to the internal wave model. The results of these methods are then compared to a numerical method to show the effectiveness of the method (Jaharuddin and Hadi (2018)). Goswami et al. (2019) looked at analytical strategies for fractional PDEs in plasma ion-acoustic waves. The hyperbolicity of multilayer SWEs that include the complete Coriolis force due to the earth's rotation was addressed by Stewart and Dellar (2013). Finite element method was used for SWEs ocean models by LeRoux et al. (1998). Busrah and Bakhtiar (2014) considered a one-and-a-half-layer model to study Kelvin waves by neglecting continuous stratification and mean currents. However, their study includes the full effects of the Earth's sphericity. Kumar (2013) uses the homotopy perturbation approach to develop a numerical solution for the coupled fractional nonlinear SWS. Several researchers have also used various strategies to evaluate differential equations from diverse perspectives and angles (Abu Arqub (2019a); Aguilar and Sutherland (2006); Momani et al. (2020a); Momani et al. (2020b); Abu Arqub (2019b); Turkyilmazoglu (2022); Turkyilmazoglu (2021); Turkyilmazoglu (2015); Turkyilmazoglu (2019); Varsoliwala and Singh (2021)).

The present research uses the modified differential transform method to study atmospheric internal wave phenomena. The motivation behind the research was to provide an efficient algorithm to solve the coupled nonlinear PDEs arising in the study of internal wave phenomena.

This paper has been organized as follows. Section 2 describes the problem statement. Section 3 discusses the implementation and convergences of MDTM. Section 4 deals with the application of MDTM to the stated problem. Numerical simulation, results, and conclusion are presented in Sections 5 and 6, respectively.

2. Problem Formulation

Based on the shallow fluid assumption, AIW is represented using a system of NLPDE. The fundamental expression of motion of fluids in the derivative form is derived from the conservation of momentum and mass. The term "shallow fluid" refers to a fluid layer with a shallow depth compared to its height. Assuming atmosphere as homogeneous fluid here whose density does not change with space and autobarotropic whose density is only determined by hydrostatic, pressure, inviscid and incompressible.The momentum equations can be given in its basic form as Warner (2010):

$$\frac{\partial \mu}{\partial \zeta} + \mu \frac{\partial \mu}{\partial \omega_1} + \rho \frac{\partial \mu}{\partial \omega_2} + q \frac{\partial \mu}{\partial \omega_3} - \mathbb{C}\rho + \frac{1}{p}\frac{\partial \rho}{\partial \omega_1} = 0, \tag{1}$$

$$\frac{\partial \rho}{\partial \zeta} + \mu \frac{\partial \rho}{\partial \omega_1} + \rho \frac{\partial \rho}{\partial \omega_2} + q \frac{\partial \rho}{\partial \omega_3} + \mathbb{C}\mu + \frac{1}{p}\frac{\partial \widetilde{\rho}}{\partial \omega_2} = 0, \tag{2}$$

$$\frac{\partial \widetilde{\rho}}{\partial \omega_3} = -\rho g. \tag{3}$$

The equation of continuity is

$$\frac{\partial p}{\partial \zeta} + p\left(\frac{\partial \mu}{\partial \omega_1} + \frac{\partial \rho}{\partial \omega_2} + \frac{\partial q}{\partial \omega_3}\right) = 0. \tag{4}$$

For homogeneous and incompressible fluid,

$$\frac{\partial p}{\partial \zeta} = 0, \tag{5}$$

so that $p = p_0$, where p_0 is a constant. Therefore, Equation (4) reduces to

$$\frac{\partial \mu}{\partial \omega_1} + \frac{\partial \rho}{\partial \omega_2} + \frac{\partial q}{\partial \omega_3} = 0. \tag{6}$$

Equation (6) is known as incompressible continuity equation. Hydrostatic equation is given by

$$\frac{\partial \widetilde{\rho}}{\partial \omega_3} = -\rho_0 g. \tag{7}$$

From Equation (7), we get

$$\frac{\partial}{\partial \omega_1}\left(\frac{\partial \widetilde{\rho}}{\partial \omega_3}\right) = \frac{\partial}{\partial \omega_3}\left(\frac{\partial \widetilde{\rho}}{\partial \omega_1}\right) = 0. \tag{8}$$

By virtue of barotropy, the vertical pressure gradient does not fluctuate horizontally, and the horizontal pressure gradient does not fluctuate vertically which is represented by Equation (8). With depth, all forces are invariable due to the wind created by the resulting Coriolis force and pressure gradient force. Integrating Equation (7) over the fluid depth, we get

$$\int_{\omega_3(\rho_B)}^{\omega_3(\rho_T)} \frac{\partial \widetilde{\rho}}{\partial \omega_3}\, d\omega_3 = -\rho_0 g \int_{\omega_3(\rho_B)}^{\omega_3(\rho_T)} d\omega_3, \tag{9}$$

where ρ_B and ρ_T denotes pressure at the bottom and top border of fluid, respectively.

$$\rho_B - \rho_T = g p_0 \vartheta, \tag{10}$$

where ϑ denotes fluid depth. If $\rho_T << \rho_B$ or $\rho_T = 0$,

$$\frac{\rho_B}{p_0} = g\vartheta,$$

$$\frac{1}{p_0}\frac{\partial \rho_B}{\partial \omega_1} = g\frac{\partial \vartheta}{\partial \omega_1}. \tag{11}$$

In Equations (1) and (2) the new expression of pressure gradient is obtained by assuming horizontal pressure gradient at the fluid base is proportional to the depth gradient. Integrate Equation (6) with respect to ω_3, the following equation is obtained:

$$\int_0^{\omega_3} \frac{\partial q}{\partial \omega_3}\, d\omega_3 = -\int_0^{\omega_3} \left(\frac{\partial \mu}{\partial \omega_3} + \frac{\partial \rho}{\partial \omega_2}\right) d\omega_3. \tag{12}$$

Because the pressure gradient is independent of ω_3, assuming ρ and μ are independent of ω_3, their derivatives are also independent of ω_3 .

$$q(\omega_3) - q(0) = -\left(\frac{\partial \mu}{\partial \omega_1} + \frac{\partial \rho}{\partial \omega_2}\right) \vartheta, \tag{13}$$

for $\omega_3 = \vartheta$. At base the vertical velocity of fluid is zero. Also

$$q(\omega_3) = \left.\frac{Dz}{D\zeta}\right|_{\vartheta} = \frac{D\vartheta}{D\zeta}. \tag{14}$$

Therefore, the equation of continuity for shallow water is given by

$$\frac{D\vartheta}{D\zeta} = -\vartheta\left(\frac{\partial \mu}{\partial \omega_1} + \frac{\partial \vartheta}{\partial \omega_2}\right). \tag{15}$$

So the three equation in terms of cartesian velocities μ, ρ and depth of the fluid ϑ are:

$$\frac{\partial \mu}{\partial \zeta} + \mu\frac{\partial \mu}{\partial \omega_1} + \rho\frac{\partial \mu}{\partial \omega_2} - \mathbb{C}\rho + g\frac{\partial \vartheta}{\partial \omega_1} = 0, \tag{16}$$

$$\frac{\partial \rho}{\partial \zeta} + \mu\frac{\partial \rho}{\partial \omega_1} + \rho\frac{\partial \rho}{\partial \omega_2} + \mathbb{C}\mu + g\frac{\partial \vartheta}{\partial \omega_2} = 0, \tag{17}$$

$$\frac{\partial \vartheta}{\partial \zeta} + \mu\frac{\partial \vartheta}{\partial \omega_1} + \rho\frac{\partial \vartheta}{\partial \omega_2} + \vartheta\left(\frac{\partial \mu}{\partial \omega_1} + \frac{\partial \rho}{\partial \omega_2}\right) = 0. \tag{18}$$

The mathematical equations in terms of μ, ρ and ϑ are considered one-dimensional as Varsoliwala and Singh (2021). We can specify a mean component for which the perturbations occur by specifying an invariant pressure gradient of the desired magnitude in the y-direction as Varsoliwala and Singh (2021). The system of equation transforms into

$$\frac{\partial \mu}{\partial \zeta} + \mu\frac{\partial \mu}{\partial \omega_1} - \mathbb{C}\rho + g\frac{\partial \vartheta}{\partial \omega_1} = 0, \tag{19}$$

$$\frac{\partial \rho}{\partial \zeta} + \mu\frac{\partial \rho}{\partial \omega_1} + \mathbb{C}\mu + g\overline{d} = 0, \tag{20}$$

$$\frac{\partial \vartheta}{\partial \zeta} + \mu\frac{\partial \vartheta}{\partial \omega_1} + \rho\overline{d} + \vartheta\frac{\partial \mu}{\partial \omega_1} = 0, \tag{21}$$

where $\omega_1, \vartheta, \mathbb{C}, \overline{d}$, g and ζ are space coordinate, depth of the fluid, Coriolis parameter, mean depth of fluid, constant of gravity and time, respectively. μ and ρ denotes the cartesian velocities, respectively.

3. Implementation of MDTM

This section discusses the method of obtaining the analytical solution and convergence of this solution obtained by MDTM. First of all, we show that the solution obtained by the proposed method exists as a power series in terms of τ or ω. Consider the following non-linear PDE:

$$v_\tau = w\left(\omega, \tau, \mu, v_\omega, v_{\omega\omega}, ...\right), \tag{22}$$

with initial condition

$$v\left(\omega, 0\right) = v_0\left(\omega\right). \tag{23}$$

Applying fundamental operation of MDTM from Table 1 to Equation (22), transformed recursive formula is given by:

$$\left(l+1\right) V_{l+1}\left(\omega\right) = W\left(\xi, v_l, \frac{dV_l\left(\omega\right)}{d\omega}, \frac{d^2V_l\left(\omega\right)}{d\omega^2}, ...\right), \tag{24}$$

and the transformed initial condition is

$$v\left(\omega\right)=v_0\left(\omega\right), \tag{25}$$

where $V_{l+1}\left(\omega\right)$ and $W\left(\omega, v_l, \frac{dV_l(\omega)}{d\omega}, \frac{d^2V_l(\omega)}{d\omega^2}, ...\right)$ are transformed forms obtained by applying MDTM to the original function $v\left(\omega,\tau\right)$ and $w\left(x,\tau,\mu,\mu_\omega,\mu_{\omega\omega},...\right)$ in the l^{th} iteration. Substituting the value of $V_l\left(\omega\right)$ for $l=0,1,2,3,4,..n$ in Equation (24), the approximate analytical series solution of Equation (22) with initial condition Equation (23) is given by

$$v\left(\omega,\tau\right)=\sum_{l=0}^{\infty}V_l\left(\omega\right)(\tau-\tau_0)^l. \tag{26}$$

The convergence of series solutions obtained by MDTM has been discussed by Moosavi Noori and Taghizadeh (2021). For specific parameter values the convergence of the series solution is discusses in Section 5.

4. Application of Modified Differential Transform Method

For analytical solution of system of Partial Differential Equations (19) through (21), we consider the following initial conditions:

$$\mu\left(\omega_1,0\right)=e^x\sec h(\omega_1)^2, \tag{27}$$

$$\rho\left(\omega_1,0\right)=2\omega_1e^{\omega_1}\sec h(2\omega_1)^2, \tag{28}$$

$$\vartheta\left(\omega_1,0\right)={\omega_1}^2\,\sec h(2\omega_1)^2. \tag{29}$$

Applying MDTM to coupled system Partial Differential Equations (19) through (21) and initial condition (27) through (29), the system of coupled recursive formula is given by

$$\left(\kappa+1\right)U_{(\kappa+1)}\left(\omega_1\right)+A_\kappa\left(\omega_1\right)-\mathbb{C}P_\kappa\left(\omega_1\right)+g\frac{\partial\nu_\kappa\left(\omega_1\right)}{\partial\omega_1}=0, \tag{30}$$

$$\left(\kappa+1\right)P_{(\kappa+1)}\left(\omega_1\right)+B_\kappa\left(\omega_1\right)-\mathbb{C}U_\kappa\left(\omega_1\right)+g\overline{d}\delta\left(k\right)=0, \tag{31}$$

$$\left(\kappa+1\right)\nu_{\kappa+1}\left(\omega_1\right)+D_\kappa\left(\omega_1\right)+\overline{d}P_\kappa\left(\omega_1\right)+E_\kappa\left(\omega_1\right)=0, \tag{32}$$

where t dimensional spectrum function $U_\kappa\left(\omega_1\right)$ and $P_\kappa\left(\omega_1\right)$ and $\nu_\kappa\left(\omega_1\right)$ denotes transformed function and $A_\kappa\left(\omega_1\right), B_\kappa\left(\omega_1\right), D_\kappa\left(\omega_1\right)$ and $E_\kappa\left(x\right)$ are transformed the function of the nonlinear terms where

$$A_\kappa\left(\omega_1\right)=\sum_{\xi=0}^{\kappa}U_\xi\left(\omega_1\right)\frac{\partial U_{\kappa-\xi}(\omega_1)}{\partial\omega_1};\;\; B_\kappa\left(\omega_1\right)=\sum_{\xi=0}^{\kappa}U_\xi\left(\omega_1\right)\frac{\partial P_{\kappa-\xi}(\omega_1)}{\partial\omega_1}\;;$$

$$D_\kappa\left(\omega_1\right)=\sum_{\xi=0}^{\kappa}U_\xi\left(\omega_1\right)\frac{\partial \nu_{\kappa-\xi}(\omega_1)}{\partial\omega_1};\; E_\kappa\left(\omega_1\right)=\sum_{\xi=0}^{\kappa}\nu_\xi\left(\omega_1\right)\frac{\partial \nu_{\kappa-\xi}}{\partial\omega_1},$$

with transformed initial condition

$$U_0\left(\omega_1\right)=e^{\omega_1}\sec h(\omega_1)^2, \tag{33}$$

$$P_0\left(\omega_1\right) = 2\omega_1\, e^{\omega_1} \sec h(2\omega_1)^2, \tag{34}$$

$$\nu_0\left(\omega_1\right) = {\omega_1}^2\ \sec h(2\omega_1)^2. \tag{35}$$

For the convenience of the reader, the first few nonlinear terms are as follows:

$$\begin{aligned}
&A_0\left(\omega_1\right) = U_0\left(\omega_1\right)\tfrac{\partial U_0(\omega_1)}{\partial\omega_1};\ A_1\left(\omega_1\right) = U_0\left(\omega_1\right)\tfrac{\partial U_1(\omega_1)}{\partial\omega_1} + U_1\left(\omega_1\right)\tfrac{\partial U_0(\omega_1)}{\partial\omega_1},\\
&A_2\left(\omega_1\right) = U_0\left(\omega_1\right)\tfrac{\partial U_2(\omega_1)}{\partial\omega_1} + U_1\left(\omega_1\right)\tfrac{\partial U_1(\omega_1)}{\partial\omega_1} + U_2\left(\omega_1\right)\tfrac{\partial U_0(\omega_1)}{\partial\omega_1},\\
&A_3\left(\omega_1\right) = U_0\left(\omega_1\right)\tfrac{\partial U_3(\omega_1)}{\partial\omega_1} + U_1\left(\omega_1\right)\tfrac{\partial U_2(\omega_1)}{\partial\omega_1} + U_2\left(\omega_1\right)\tfrac{\partial U_1(\omega_1)}{\partial\omega_1} + U_3\left(\omega_1\right)\tfrac{\partial U_0(\omega_1)}{\partial\omega_1},\\
&B_0\left(\omega_1\right) = U_0\left(\omega_1\right)\tfrac{\partial P_0(\omega_1)}{\partial\omega_1};\ B_1\left(\omega_1\right) = U_0\left(\omega_1\right)\tfrac{\partial P_1(\omega_1)}{\partial\omega_1} + U_1\left(\omega_1\right)\tfrac{\partial P_0(\omega_1)}{\partial\omega_1},\\
&B_2\left(\omega_1\right) = U_0\left(\omega_1\right)\tfrac{\partial P_2(\omega_1)}{\partial\omega_1} + U_1\left(\omega_1\right)\tfrac{\partial P_1(\omega_1)}{\partial\omega_1} + U_2\left(\omega_1\right)\tfrac{\partial P_0(\omega_1)}{\partial\omega_1},\\
&B_3\left(\omega_1\right) = U_0\left(\omega_1\right)\tfrac{\partial P_3(\omega_1)}{\partial\omega_1} + U_1\left(\omega_1\right)\tfrac{\partial P_2(\omega_1)}{\partial\omega_1} + U_2\left(\omega_1\right)\tfrac{\partial P_1(\omega_1)}{\partial\omega_1} + U_3\left(x\omega_1\right)\tfrac{\partial p_0(\omega_1)}{\partial\omega_1},\\
&D_0\left(\omega_1\right) = U_0\left(\omega_1\right)\tfrac{\partial \nu_0(\omega_1)}{\partial\omega_1};\ D_1\left(\omega_1\right) = U_0\left(\omega_1\right)\tfrac{\partial \nu_1(\omega_1)}{\partial\omega_1} + U_1\left(\omega_1\right)\tfrac{\partial \nu_0(\omega_1)}{\partial\omega_1},\\
&D_2\left(\omega_1\right) = U_0\left(\omega_1\right)\tfrac{\partial \nu_2(\omega_1)}{\partial\omega_1} + U_1\left(\omega_1\right)\tfrac{\partial \nu_1(\omega_1)}{\partial\omega_1} + U_2\left(\omega_1\right)\tfrac{\partial \nu_0(\omega_1)}{\partial\omega_1},\\
&D_3\left(\omega_1\right) = U_0\left(\omega_1\right)\tfrac{\partial \nu_3(\omega_1)}{\partial\omega_1} + U_1\left(\omega_1\right)\tfrac{\partial \nu_2(\omega_1)}{\partial\omega_1} + U_2\left(\omega_1\right)\tfrac{\partial \nu_1(\omega_1)}{\partial\omega_1} + U_3\left(\omega_1\right)\tfrac{\partial \nu_0(\omega_1)}{\partial\omega_1},\\
&E_0\left(\omega_1\right) = \nu_0\left(\omega_1\right)\tfrac{\partial \nu_0(\omega_1)}{\partial\omega_1};\ E_1\left(\omega_1\right) = \nu_0\left(\omega_1\right)\tfrac{\partial \nu_1(\omega_1)}{\partial\omega_1} + \nu_1\left(\omega_1\right)\tfrac{\partial \nu_0(\omega_1)}{\partial\omega_1},\\
&E_2\left(\omega_1\right) = \nu_0\left(\omega_1\right)\tfrac{\partial \nu_2(\omega_1)}{\partial\omega_1} + \nu_1\left(\omega_1\right)\tfrac{\partial \nu_1(\omega_1)}{\partial\omega_1} + \nu_2\left(\omega_1\right)\tfrac{\partial \nu_0(\omega_1)}{\partial\omega_1},\\
&E_3\left(\omega_1\right) = \nu_0\left(\omega_1\right)\tfrac{\partial \nu_3(\omega_1)}{\partial\omega_1} + \nu_1\left(\omega_1\right)\tfrac{\partial \nu_2(\omega_1)}{\partial\omega_1} + \nu_2\left(\omega_1\right)\tfrac{\partial \nu_1(\omega_1)}{\partial\omega_1} + \nu_3\left(\omega_1\right)\tfrac{\partial \nu_0(x)}{\partial\omega_1}.
\end{aligned}$$

Substituting Equations (33) and (34) into Equations (30) through (34), we obtain the coefficients of the series solution as:

$$U_1\left(\omega_1\right) = \frac{2f\omega_1}{\xi_1^2} - \frac{e^{\omega_1}}{\xi_2^2}\left(\frac{e^{\omega_1}}{\xi_2^2} - \frac{2e^{\omega_1}\xi_4}{\xi_2^3}\right) - g\left(\frac{2\omega_1}{\xi_1^2} - \frac{4x^2\xi_3}{\xi_1^3}\right),$$

$$P_1\left(\omega_1\right) = -Hg - \frac{e^{\omega_1}}{\xi_2^2}\left(\frac{2}{\xi_1^2} - \frac{8\omega_1\xi_3}{\xi_2^3}\right) - \frac{fe^{\omega_1}}{\xi_1^2},$$

$$\nu_1\left(\omega_1\right) = -\frac{{\omega_1}^2}{\xi_1^2}\left(\frac{e^{\omega_1}}{\xi_2^2} - \frac{2e^{\omega_1}\xi_3}{\xi_2^2}\right) - \frac{e^{\omega_1}}{\xi_2^2}\left(\frac{2\omega_1}{\xi_1^2} - \frac{4\omega_1^2\xi_3}{\xi_1^3}\right) - \frac{2H\omega_1}{\xi_1^2},$$

where $\cosh\left(2\omega_1\right) = \xi_1$, $\cosh\left(\omega_1\right) = \xi_2$, $\sinh\ (2\omega_1) = \xi_3$, $\sinh\ (\omega_1) = \xi_4$. The coefficients are calculated up to the fifth iteration, but only the first iteration is mentioned as the remaining iteration are too long to mention. Applying inverse transformations for the set of values $\left\{U_k\left(\omega_1\right)\right\}_{\kappa=0}^{n}$,$\left\{P_k\left(\omega_1\right)\right\}_{\kappa=0}^{n}$ and $\left\{\vartheta_k\left(\omega_1\right)\right\}_{\kappa=0}^{n}$ gives an n-term approximation analytical solution as follows:

$$\mu\left(\omega_1,\zeta\right) = \sum_{\kappa=0}^{n} U_\kappa\left(\omega_1\right)\zeta^\kappa,$$

$$\mu\left(\omega_1,\zeta\right) = \frac{e^{\omega_1}}{\xi_2^2} + \left(\frac{2f\omega_1}{\xi_1^2} - \frac{e^{\omega_1}}{\xi_2^2}\left(\frac{e^{\omega_1}}{\xi_2^2} - \frac{2e^{\omega_1}\xi_4}{\xi_1^3}\right) - g\left(\frac{2\omega_1}{\xi_1^2} - \frac{4x^2\xi_3}{\xi_1^3}\right)\right)\zeta + \ldots \tag{36}$$

$$\rho\left(\omega_1,\zeta\right) = \sum_{\kappa=0}^{n} P_\kappa\left(\omega_1\right)\zeta^\kappa,$$

$$\rho\left(\omega_1,\zeta\right)=\frac{2\omega_1\,e^{\omega_1}}{\xi_1^2}+\left(-Hg-\frac{e^{\omega_1}}{\xi_2^2}\left(\frac{2}{\xi_1^2}-\frac{8\omega_1\xi_3}{\xi_2^3}\right)-\frac{fe^{\omega_1}}{\xi_1^2}\right)\zeta+...,\tag{37}$$

$$\vartheta\left(\omega_1,\zeta\right)=\sum_{\kappa=0}^{n}\nu_\kappa\left(\omega_1\right)\zeta^\kappa,$$

$$\vartheta\left(\omega_1,\zeta\right)=\frac{{\omega_1}^2}{\xi_1^2}+\left(-\frac{{\omega_1}^2}{\xi_1^2}\left(\frac{e^{\omega_1}}{\xi_2^2}-\frac{2e^{\omega_1}\xi_3}{\xi_2^2}\right)-\frac{e^{\omega_1}}{\xi_2^2}\left(\frac{2\omega_1}{\xi_1^2}-\frac{4\omega_1^2\xi_3}{\xi_1^3}\right)-\frac{2H\omega_1}{\xi_1^2}\right)\zeta+....\tag{38}$$

5. Result and Discussion

This section discusses the analytical approximated solution of the stated problem represented by Equations (19) through (21) with initial condition (27) through (29) using MATLAB software package with following parameter values as Busrah and Bakhtiar (2014): $\mathbb{C}=2\Omega\sin\alpha$ where $\Omega=7.29\times10^{-5}\,rad/s$ and $\alpha=\frac{\pi}{3}$, $g=9.8$, $\overline{d}=-\frac{\mathbb{C}}{g}\overline{U}$, where $\overline{U}=2.5$ m/s. The semi-analytical solution using the mention parameter values is given by:

$$\mu\left(\omega_1,\zeta\right)=\frac{e^{\omega_1}}{\xi_2^2}-\zeta\left(\frac{1807757627164716012183\,\omega_1}{92233720368547758080\,\xi_1^2}+\frac{\mathrm{e}^{2\,\omega_1}}{\xi_2^4}-\frac{196\,\omega_1^2\,\xi_2^2}{5\,\xi_2^3}\right)+...,\tag{39}$$

$$\rho\left(\omega_1,\zeta\right)=\frac{\left(11646029410023092\,\zeta\,\xi_2^2-4658411764009237\,\zeta\,\mathrm{e}^{\omega_1}\right)\xi_1^2+\zeta}{36893488147419103232\,\xi_1^2\,\xi_2^2}+...,\tag{40}$$

$$\vartheta\left(\omega_1,\zeta\right)=\frac{\omega_1^2\,\zeta}{\xi_1^2}+\frac{\omega_1\,\zeta\,\left(297092586990385\;\xi_2^2-9223372036854775808\;\omega_1\,\mathrm{e}^{\omega_1}\right)}{4611686018427387904\,\xi_1^2\,\xi_2^2}+...,\tag{41}$$

where $\zeta=7.3786976294838206464\left(\omega_1\,\xi_2^2-\zeta\,\omega_1\,\mathrm{e}^{\omega_1}\right)$. For convergence analysis according to theorem and corollary as Warner (2010), we have

$$\Psi_{0,\mu}=\frac{\|\sigma_1\|}{\|\sigma_0\|}=0.4556<1,$$

$$\Psi_{0,\rho}=\frac{\|\sigma_1\|}{\|\sigma_0\|}=0.4676<1,$$

$$\Psi_{0,\vartheta}=\frac{\|\sigma_1\|}{\|\sigma_0\|}=0.4776<1,$$

$$\Psi_{1,\mu}=\frac{\|\sigma_1\|}{\|\sigma_0\|}=0.3425<1,$$

$$\Psi_{1,\rho}=\frac{\|\sigma_1\|}{\|\sigma_0\|}=0.3645<1,$$

$$\Psi_{1,\vartheta}=\frac{\|\sigma_1\|}{\|\sigma_0\|}=0.3348<1,$$

$$\vdots$$

and so on. Hence, $\sum\limits_{\kappa=0}^{n} U_\kappa(\omega_1)\zeta^\kappa$, $\sum\limits_{\kappa=0}^{n} P_\kappa(\omega_1)\zeta^\kappa$, $\sum\limits_{\kappa=0}^{n} \nu_\kappa(\omega_1)\zeta^\kappa$ are convergent. Tables 1, 2, 3 gives numerical values for the vertical velocity component (ρ), horizontal velocity component (μ), and depth (ϑ) for $0 \leqslant \zeta \leqslant 0.1$ and $0 \leqslant \omega_1 \leqslant 2$. Table 2 also shows that values are very modest in contrast to horizontal velocity component and vertical velocity component, which is consistent with the AIWs phenomena, in which the fluid's depth is insignificant in comparison to its horizontal scale. The behaviour of velocity component (ρ), horizontal velocity component (μ), and depth (ϑ) with respect to space (ω_1) and time (ζ) is presented in Figures 1, 2, and 3. The solution obtained by MDTM is compared with HAM and EADM graphical and numerical in Figures 6, 7, 8 and Tables 4, 5, 6, respectively, which shows that the results obtain using MDTM shows a good agreement with other existing methods. Figure 4 represents that the velocity component, horizontal velocity component, and depth at $\zeta = 0.04$ and $0 \leqslant \omega_1 \leqslant 2$ decreases as distance increases. Figure 5 represents that the velocity component, horizontal velocity component, and depth at $\omega_1 = 1$ and $0 \leqslant \zeta \leqslant 0.1$ changes slow for the fixed distance as time increases.

6. Conclusion

In this research Modified differentiable transform is successfully applied to obtain the series solution of internal wave phenomena with its convergence criteria. The comparison of the obtained solution by MDTM with other existing methods shows an excellent agreement. It proves that MDTM is a promising tool for dealing with an extensive system of coupled PDE with non linearity as it does require linearization, perturbation, discretization, or calculation of unneeded terms like adomain polynomial. The straightforward applicability and efficiency of converting the nonlinear terms into an algebraic system is a significant advantage of MDTM over methods. The findings demonstrate that the MDTM is an effective mathematical tool for dealing with the mathematical model described by an extensive system of PDE.

Acknowledgment:

The authors would like to express their thanks to the editor and anonymous reviewers for carefully reading the paper and giving their valuable suggestion to improve the paper.

REFERENCES

Abu Arqub, O. (2019a). Application of residual power series method for the solution of time-fractional Schrodinger equations in one-dimensional space, Fundamenta Informaticae, Vol. 166, Issue 2, pp. 87–110.

Abu Arqub, O. (2019b). Computational algorithm for solving singular Fredholm time-fractional partial integrodifferential equations with error estimates, Journal of Applied Mathematics and Computing, Vol. 59, Issue 1, pp. 227–243.

Aguilar, D. A., and Sutherland, B. R. (2006). Internal wave generation from rough topography, Physics of Fluids, Vol. 18, Issue 06, pp. 1-33.

Boyd, J. P., and Zhou, C. (2008). Kelvin waves in the nonlinear shallow water equations on the sphere: Nonlinear travelling waves and the corner wave bifurcation, Journal of Fluid Mechanics, Vol. 617, Issue 1, pp. 187–205.

Busrah, Z. and Bakhtiar, T. (2014). Application of Homotopy and Variational Iteration Methods to the Atmospheric Internal Waves Model, IOSR Journal of Mathematics, Vol. 10, Issue 5, pp. 46-53.

Goswami, A., Singh, J., Kumar, D., and Gupta, S. (2019). An efficient analytical technique for fractional partial differential equations occurring in ion acoustic waves in plasma, Journal of Ocean Engineering and Science, Vol. 4, Issue 2, pp. 85-99.

Imani, A. A., Ganji, D. D., Rokni, H. B., Latifizadeh, H., Hesameddini, E., and Rafiee, M. H. (2012). Approximate traveling wave solution for shallow water wave equation, Applied Mathematical Modelling, Vol. 36, Issue 4, pp. 1550-1557.

Jaharuddin and Hadi Hermansyah. (2018). Analytical approach for solving the internal waves problems involving the tidal force, Journal of Applied Mathematics, Vol. 2018, Issue 12, pp. 1-6.

Karunakar, P. and Chakraverty, S. (2018). Solving shallow water equations with crisp and uncertain initial conditions, International Journal of Numerical Methods for Heat & Fluid Flow, Vol. 28, Issue 12, pp. 2801-2815.

Karunakar, P. and Chakraverty, S. (2018). Homotopy perturbation method for predicting tsunami wave propagation with crisp and uncertain parameters, International Journal of Numerical Methods for Heat & Fluid Flow, Vol. 31, Issue 01, pp. 92-105.

Kumar, S. (2013). A numerical study for the solution of time fractional nonlinear shallow water equation in oceans, Zeitschrift fur Naturforschung A, Vol. 68, Issue 8, pp. 547-553.

Le Roux, D. Y., Staniforth, A., and Lin, C. A. (1998). Finite elements for shallow-water equation ocean models, Monthly Weather Review, Vol. 126, Issue 7, pp. 1931-1951.

Momani, S., Abu Arqub, O. and Maayah, B. (2020a). Piecewise optimal fractional reproducing kernel solution and convergence analysis for the atangana baleanu caputo model of the Lienard's equation, Fractals, Vol. 28, Issue 8, pp. 1-13.

Momani, S., Abu Arqub, O. and Maayah, B. (2020b). The reproducing kernel algorithm for numerical solution of Van der Pol damping model in view of the Atangana Baleanu fractional approach, Vol. 28, Issue 8, pp. 1-12.

Moosavi Noori, S. R. and Taghizadeh, N. (2021). Study of convergence of reduced differential transform method for different classes of differential equations, International Journal of Differential Equations, Vol. 2021, Issue 1, pp. 1-16.

Stewart, A. L. and Dellar, P. J. (2013). Multilayer shallow water equations with complete Coriolis force. Part 3. Hyperbolicity and stability under shear, Journal of Fluid Mechanics, Vol. 723, Issue 6, pp. 289–317.

Turkyilmazoglu, M. (2015). Is homotopy perturbation method the traditional Taylor series expansion, Hacettepe Journal of Mathematics and Statistics, Vol. 44, Issue 3, pp. 651-657.

Turkyilmazoglu, M. (2019). Equivalence of ratio and residual approaches in the homotopy analysis method and some applications in nonlinear science and engineering, Computer Modeling in Engineering & Sciences, Vol. 120, Issue 1, pp. 63-81.

Turkyilmazoglu, M. (2021). Nonlinear problems via a convergence accelerated decomposition method of Adomian, Vol. 127, Issue 1, pp. 1-22.

Turkyilmazoglu, M. (2022). Maximum wave run-up over beaches of convex/concave bottom profiles, Continental Shelf Research, Vol. 232, Issue 2022, pp. 1-8.

Varsoliwala, A. C. and Singh, T. R. (2022). Mathematical modelling of atmospheric internal waves phenomenon and its solution by Elzaki Adomian decomposition method, Journal of Ocean Engineering and Science, Vol. 7, Issue 3, pp. 203–212.

Warner, T. T. (2010). *Numerical Weather and Climate Prediction*, National Center for Atmospheric Research and the University of Colorado, Colorado.

Table 1. Solution $\mu(\omega_1, \zeta)$ for different values of ω_1 and ζ

ω_1	$\zeta = 0$	$\zeta = 0.02$	$\zeta = 0.04$	$\zeta = 0.06$	$\zeta = 0.08$	$\zeta = 0.1$
0.2	1.17382055010529	1.10394648990523	1.04281789464098	0.99136570893583	0.94950868550835	0.91674541915434
0.4	1.27646307333570	1.22235739039917	1.16040745259023	1.09444941308803	1.02754727241215	0.96097450445032
0.6	1.29657921914999	1.29338429348215	1.27816448289798	1.25114567886057	1.21451365832879	1.17299971931881
0.8	1.24420015707333	1.27481382026098	1.30016517300075	1.31797019885855	1.32567195588917	1.32050656680318
1	1.14160862122846	1.18150497823164	1.22205731352074	1.26229633115233	1.30079538924922	1.33557284222827
1.2	1.01270205118126	1.04834601765969	1.08652111046652	1.12729484543237	1.17064595005641	1.21643580085099
1.4	0.87654144467375	0.90376846210306	0.93325479177443	0.96527567923920	1.00014081381955	1.03819678929355
1.6	0.74556548727735	0.76472758769768	0.78538552066967	0.80773500380157	0.83200537056795	0.85846427108557
1.8	0.62649165491863	0.63936785165778	0.65310902874133	0.66781667447176	0.68360867583633	0.70062157564331
2	0.52204290827576	0.53047118574834	0.53936456682840	0.54876879146602	0.55873594368095	0.56932524133422

Table 2. Solution $\rho(x, t)$ for different values of ω_1 and ζ

ω_1	$\zeta = 0$	$\zeta = 0.02$	$\zeta = 0.04$	$\zeta = 0.06$	$\zeta = 0.08$	$\zeta = 0.1$
0.2	0.342255514432471	0.313623748739862	0.283991520834054	0.253612276622892	0.222379605437395	0.189813424336102
0.4	0.447244134185795	0.447447980351848	0.444639583498955	0.439219849118303	0.431786048670346	0.423089002447617
0.6	0.366023995448891	0.381509278376572	0.395974056917585	0.408959188533379	0.420086503530180	0.429120283859302
0.8	0.240843321309257	0.255922360902292	0.271859772678012	0.288451476714494	0.305376600810571	0.322174933642583
1	0.141301649706329	0.150991750162516	0.161687434019689	0.173473451445028	0.186419338645104	0.200572011316873
1.2	0.077721058419163	0.082873363926876	0.088612621060336	0.095029782483018	0.102230318391243	0.110335724429274
1.4	0.041111462288953	0.043581889668243	0.046316026855938	0.049356527567586	0.052754510575690	0.056570843373782
1.6	0.021197433077131	0.022311857957907	0.023529931071703	0.024866762278598	0.026340310168196	0.027971811179474
1.8	0.010734800757347	0.011219516693992	0.011741981118016	0.012306852343560	0.012919553733266	0.013586379539330
2	0.005363802732104	0.005570817313895	0.005790957104495	0.006025552230860	0.006276115218673	0.006544363289885

Table 3. Solution $\vartheta(\omega_1, \zeta)$ for different values of ω_1 and ζ

ω_1	$\zeta = 0$	$\zeta = 0.02$	$\zeta = 0.04$	$\zeta = 0.06$	$\zeta = 0.08$	$\zeta = 0.1$
0.2	0.0342255514432471	0.0274458486055882	0.0216857543766980	0.0168577809456019	0.0128968012768440	0.0098819546460326
0.4	0.0894488268371590	0.0831695780620673	0.0764439388004842	0.0696831910382803	0.0631105102002532	0.0566189567601499
0.6	0.1098071986346670	0.1094082813911880	0.1077291332717650	0.1048335781975410	0.1010336422944210	0.0969618948653115
0.8	0.0963373285237027	0.0998117973438979	0.1028161212228780	0.1050806123956170	0.1062928639661910	0.1061031087519420
1	0.0706508248531645	0.0746025481752057	0.0787472424397094	0.0830030241438369	0.0872375247860272	0.0912558966878234
1.2	0.0466326350514979	0.0495433954424299	0.0527494162112457	0.0562772160443726	0.0601496261679602	0.0643837248154856
1.4	0.0287780236022672	0.0305374343626966	0.0324911137852941	0.0346696704906922	0.0371090894952830	0.0398514114818826
1.6	0.0169579464617045	0.0179074164271985	0.0189541591644014	0.0201135393561632	0.0214039644676739	0.0228473520737857
1.8	0.0096613206816125	0.0101379533742486	0.0106569619948070	0.0112242407982366	0.0118467509323820	0.0125326770588064
2	0.0053638027321036	0.0055915515453541	0.0058363092411512	0.0061000520301792	0.0063850611021316	0.0066939629051971

Table 4. Comparison of $\mu(\omega_1, \zeta)$ for the different values of ω_1 and ζ

ω_1	$\zeta = 0$			$\zeta = 0.02$			$\zeta = 0.04$		
	HAM	**EADM**	**MDTM**	**HAM**	**EADM**	**RDTM**	**HAM**	**EADM**	**RDTM**
0	1.000000	1.000000	1.00000000000000	0.983500	0.980000	0.98768903966591	0.967000	0.960000	0.98957666986782
0.2	1.173820	1.173820	1.17382055010529	1.113130	1.100260	1.10394648990523	1.052440	1.026690	1.04281789464098
0.4	1.276460	1.276460	1.27646307333570	1.236110	1.227550	1.22235739039917	1.195750	1.178630	1.16040745259023
0.6	1.296580	1.296580	1.29657921914999	1.298660	1.299100	1.29338429348215	1.300740	1.301620	1.27816448289798
0.8	1.244200	1.244200	1.24420015707333	1.271070	1.276770	1.27481382026098	1.297930	1.309330	1.30016517300075
1	1.141610	1.141610	1.14160862122846	1.174060	1.180950	1.18150497823164	1.206520	1.220290	1.22205731352074
1.2	1.012700	1.012700	1.01270205118126	1.041100	1.047120	1.04834601765969	1.069490	1.081540	1.08652111046652
1.4	0.876541	0.876541	0.87654144467375	0.898141	0.902722	0.90376846210306	0.919740	0.928903	0.93325479177443
1.6	0.745565	0.745565	0.74556548727735	0.760805	0.764037	0.76472758769768	0.776044	0.782509	0.78538552066967
1.8	0.626492	0.626492	0.62649165491863	0.636783	0.638966	0.63936785165778	0.647074	0.651439	0.65310902874133
2	0.522043	0.522043	0.52204290827576	0.528816	0.530252	0.53047118574834	0.535589	0.538462	0.53936456682840

Table 5. Comparison of $\rho\left(\omega_1, \zeta\right)$ for the different values of ω_1 and ζ

ω_1	$\zeta=0$			$\zeta=0.02$			$\zeta=0.04$		
	HAM	**EADM**	**RDTM**	**HAM**	**EADM**	**RDTM**	**HAM**	**EADM**	**MDTM**
0	0.0000000	0.0000000	0.0000000000000000	0.00000000	0.00000000	0.0003803170821522	0.00000000	0.00000000	0.0000000000000000
0.2	0.0342256	0.0342256	0.0342255514432471	0.02820320	0.02692570	0.0274458486055882	0.22180080	0.0196258	0.0216857543766980
0.4	0.0894488	0.0894488	0.0894488268371590	0.08458110	0.08354850	0.0831695780620673	0.07971330	0.7764820	0.0764439388004842
0.6	0.1098070	0.1098070	0.1098071986346670	0.10998400	0.11002200	0.1094082813911880	0.11016200	0.1102370	0.1077291332717650
0.8	0.0963373	0.0963373	0.0963373285237027	0.09933320	0.09996870	0.0998117973438979	0.10232900	0.1036000	0.1028161212228780
1	0.0706508	0.0706508	0.0706508248531645	0.73817300	0.07448900	0.0746025481752057	0.07698380	0.0783272	0.0787472424397094
1.2	0.0466326	0.0466326	0.0466326350514979	0.04891990	0.04940510	0.0495433954424299	0.05120720	0.0521776	0.0527494162112457
1.4	0.0287780	0.0287780	0.0287780236022672	0.03015680	0.03044930	0.0305374343626966	0.03153560	0.3212060	0.0324911137852941
1.6	0.0169579	0.0169579	0.0169579464617045	0.01770480	0.01786320	0.0179074164271985	0.01845170	0.0187685	0.0189541591644014
1.8	0.0096613	0.0096613	0.0096613206816125	0.01003850	0.01011850	0.0101379533742486	0.01041570	0.0105757	0.0106569619948070
2	0.0053638	0.0053638	0.0053638027321036	0.00554517	0.00558364	0.0055915515453541	0.00572653	0.0058035	0.0058363092411512

Table 6. Comparison of $\vartheta\left(\omega_1, \zeta\right)$ for the different values of ω_1 and ζ

ω_1	$\zeta=0$			$\zeta=0.02$			$\zeta=0.04$		
	HAM	**EADM**	**RDTM**	**HAM**	**EADM**	**RDTM**	**HAM**	**EADM**	**MDTM**
0	0.0000000	0.0000000	0.00000000000000	-0.0329969	-0.0329962	-0.039292517272731	-0.0659938	-0.0799924	-0.077521787737289
0.2	0.3422560	0.3422560	0.34225551443247	0.3191890	0.3142960	0.313623748739862	0.2961220	0.2863369	0.283991520834054
0.4	0.4472440	0.4472440	0.44724413418580	0.4487180	0.4490300	0.447447980351848	0.4501930	0.4508160	0.444639583498955
0.6	0.3660240	0.3660240	0.36602399544889	0.3790890	0.3818590	0.381509278376572	0.3921540	0.3976930	0.395974056917585
0.8	0.2408430	0.2408430	0.24084332130926	0.2528960	0.2554500	0.255922360902292	0.2649480	0.2700560	0.271859772678012
1	0.1413020	0.1413020	0.14130164970633	0.1489080	0.1505200	0.150991750162516	0.1565150	0.1597370	0.161687434019689
1.2	0.0777211	0.0777211	0.07772105841916	0.0817537	0.0826069	0.082873363926876	0.0857864	0.0874927	0.088612621060336
1.4	0.0411115	0.0411115	0.04111146228895	0.0430527	0.0434624	0.043581889668243	0.0449939	0.0458133	0.046316026855938
1.6	0.0211974	0.0211974	0.02119743307713	0.2207920	0.0226440	0.022311857957907	0.0229610	0.0233315	0.023529931071703
1.8	0.0107348	0.0107348	0.01073480075735	0.1112150	0.0112020	0.011219516693992	0.0115083	0.0116692	0.011741981118016
2	0.0053638	0.0053638	0.00536380273210	0.0055306	0.0055647	0.005570817313895	0.0056974	0.0057655	0.005790957104495

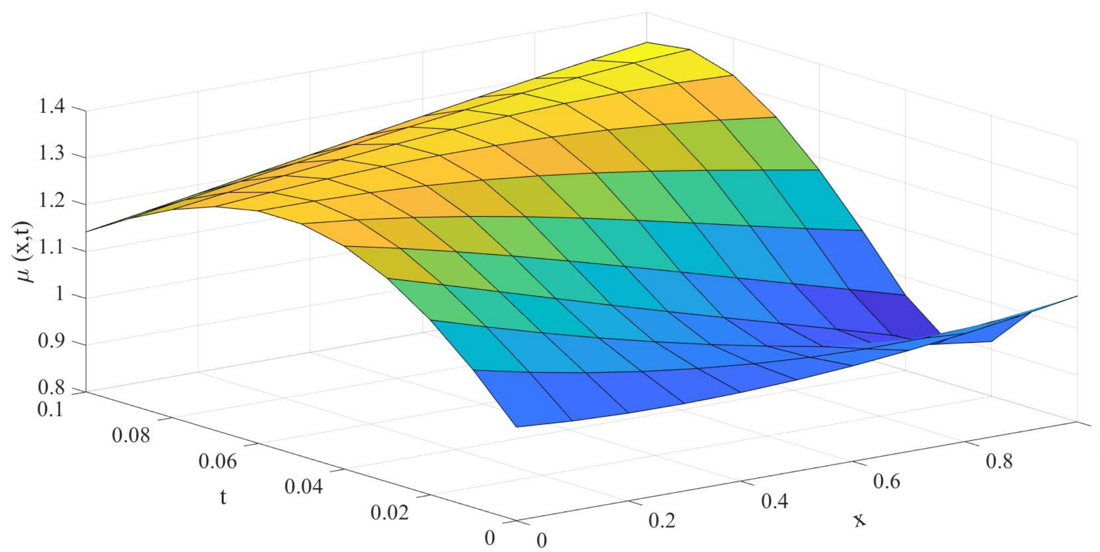

Figure 1. Analytical result for $\rho\,(x,t)$ with parameter values $\Omega = 7.29 \times 10^{-5}\, rad/s$,$\alpha = \frac{\pi}{3}$, $g = 9.8$, $\overline{U} = 2.5$ m/s

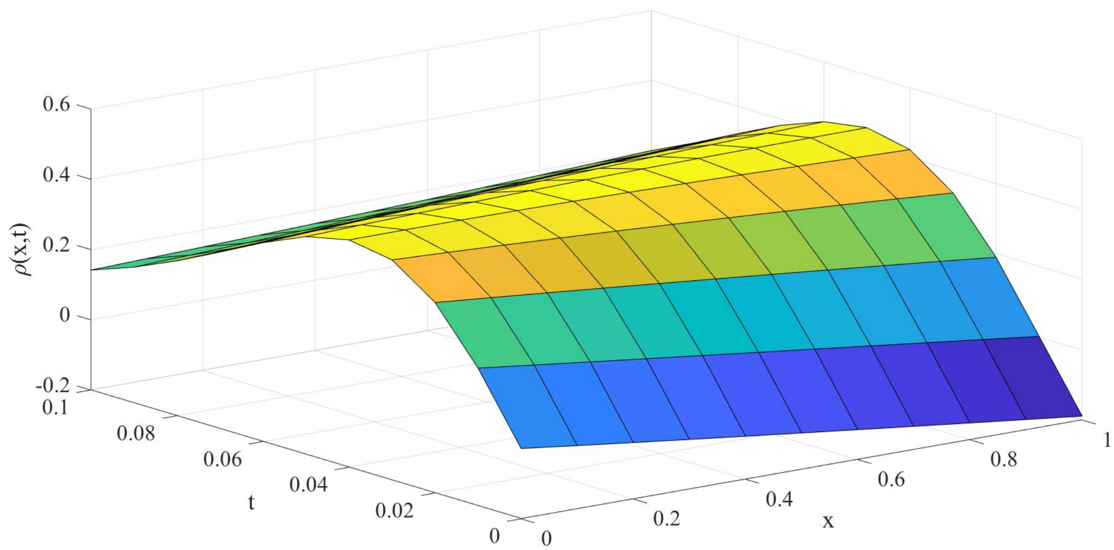

Figure 2. Analytical result for $\mu\left(x,t\right)$ with parameter values $\Omega = 7.29 \times 10^{-5}\, rad/s$,$\alpha = \frac{\pi}{3}$, $g = 9.8$, $\overline{U} = 2.5$ m/s

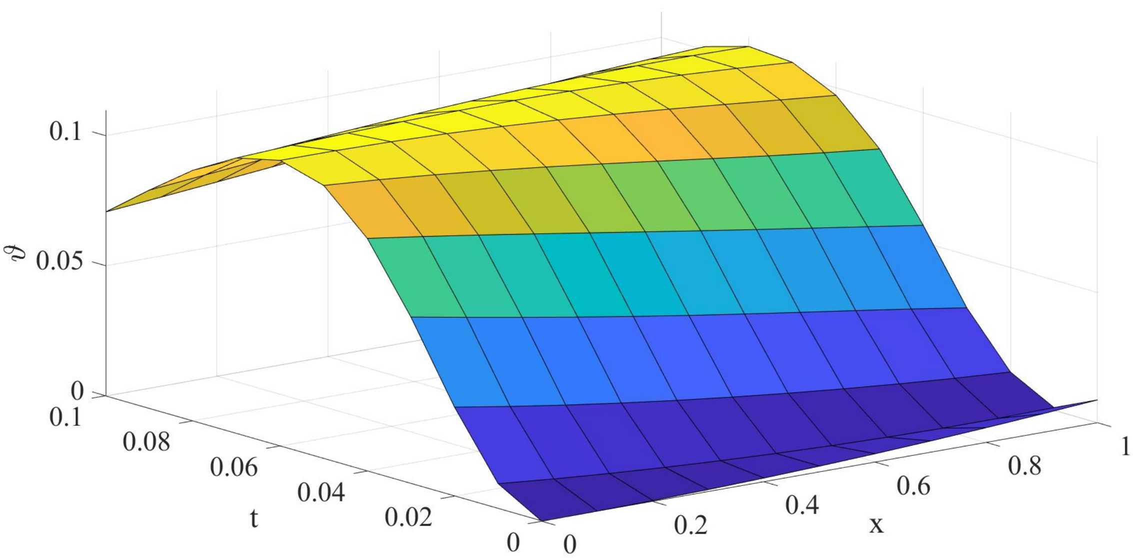

Figure 3. Analytical result for $\vartheta\left(x,t\right)$ with parameter values $\Omega = 7.29 \times 10^{-5}\, rad/s$,$\alpha = \frac{\pi}{3}$, $g = 9.8$, $\overline{U} = 2.5$ m/s

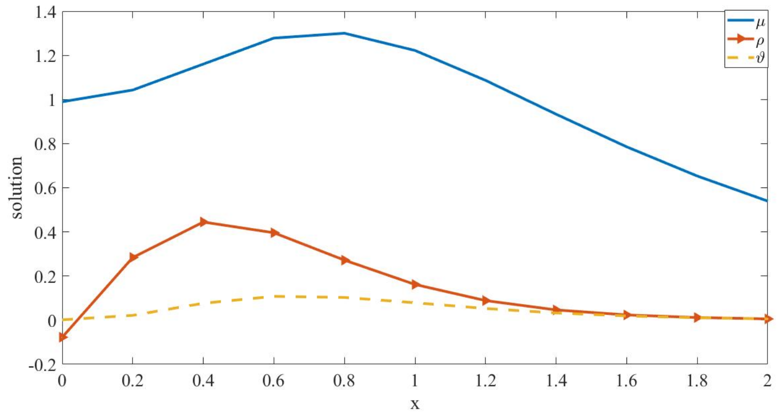

Figure 4. Analytical approximate solution of μ, ρ, ϑ for $\zeta = 0.04$ and $0 \leqslant \omega_1 \leqslant 2$

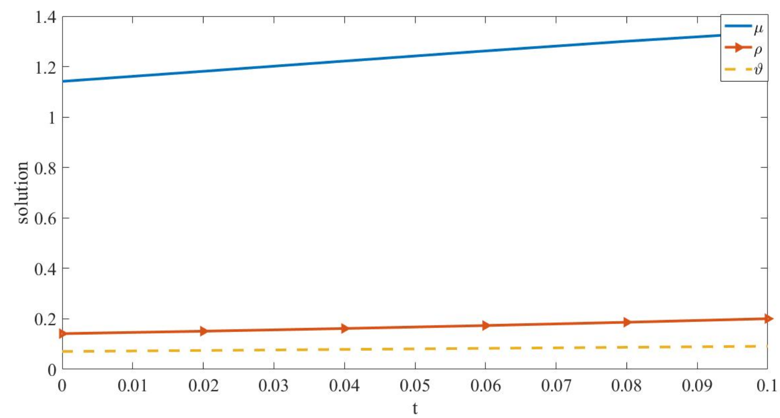

Figure 5. Analytical approximate solution of μ, ρ, ϑ for $\omega_1 = 1$ and $0 \leqslant t \leqslant 0.1$

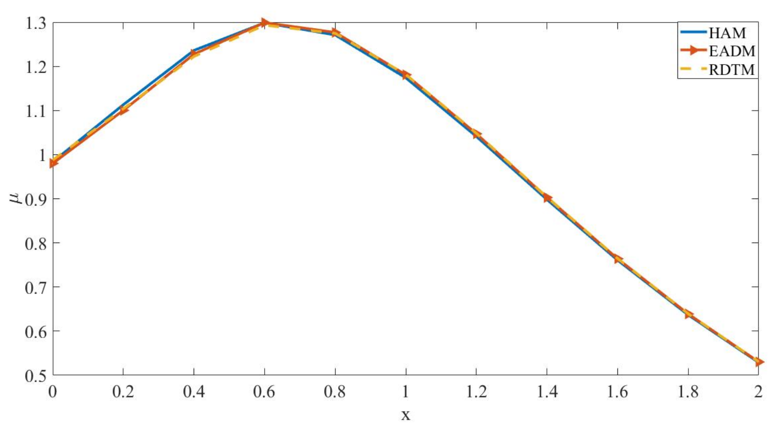

Figure 6. Comparison of analytical approximate solution of μ for $\zeta = 0.04$ and $0 \leqslant \omega_1 \leqslant 2$

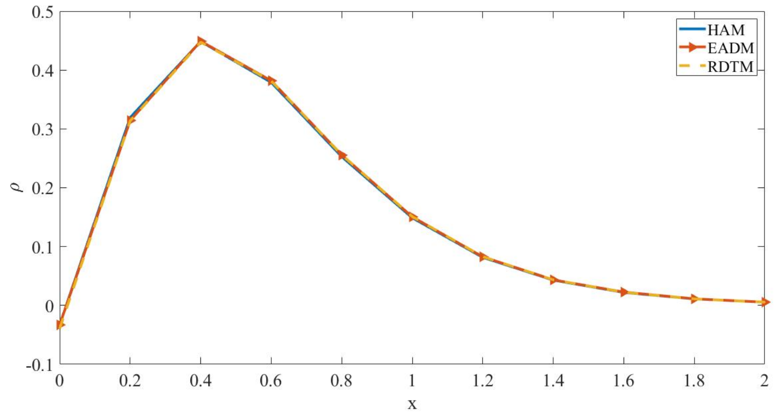

Figure 7. Comparison of analytical approximate solution of ρ for $\zeta = 0.04$ and $0 \leqslant \omega_1 \leqslant 2$

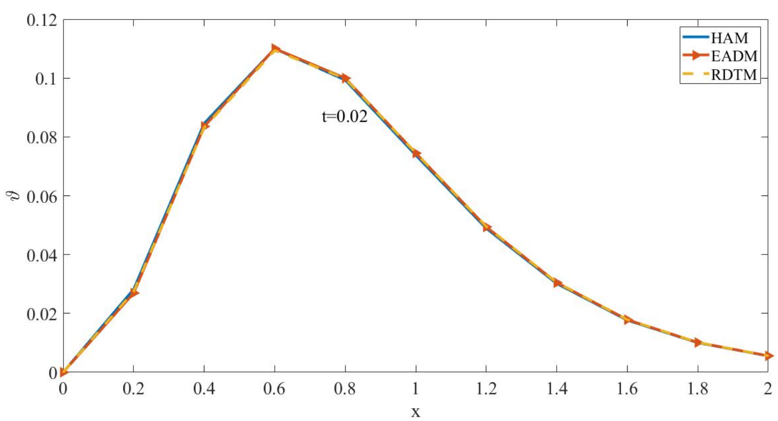

Figure 8. Comparison of analytical approximate solution of ϑ for $\zeta = 0.04$ and $0 \leqslant \omega_1 \leqslant 2$